NIPES Journal of Science and Technology Research 4(4) 2022 pp.107 – 121 pISSN-2682-5821, eISSN-2682-5821

Journal of Science and Technology Research

Journal homepage: www.nipesjournals.org.ng

Performance Evaluation of A PV Solar Tracker Panel

***Oriaifo A. P. and Akahomen I. E.**

Department of Electrical/Electronic Engineering, Faculty of Engineering, University of Benin, PMB 1154, Benin City, Nigeria.

*patrick.oriaifo@uniben.edu; itakahomen@gmail.com

ARTICLE INFORMATION

Keywords: *Solar trackers, ATMEGA328P, LDRs, PV solar panels, servo motors, efficiency*

Article history:

Received 23 July 2022
Revised 15 September 2022
Accepted 16 September 2022
Available online 6 December 2022

https://doi.org/*10.5281/zenodo.7406286*

ABSTRACT

Solar energy is the most abundant source of renewable energy and solar panels are used to convert it to electrical energy in homes and industries but fixed panels are not efficient in maximizing the amount of the sun's radiation it receives hence, the use of solar trackers. This paper presents the evaluation and comparison of the performance of the solar tracker panel over the fixed panels. The designed solar tracker is microcontroller-based using ATMEGA328P, ESF-12F module, light-dependent resistors (LDRs), servo motors, a liquid crystal display (LCD) and solar panels. The experiment was carried out for 20 days between 8 am and 6 pm from the 20th of May to the 9th of June 2021. It was observed that the efficiency of the solar tracker panel outperformed the fixed panel by approximately 43% overall. However, the difference in performance was significant on sunny days compared to cloudy and rainy days.

1. Introduction

Energy is a prime factor in the development of a nation. An enormous amount of energy is extracted, distributed, converted, and consumed in the global society daily [1]. 85% of energy production is dependent on fossil fuels. The resources of fossil fuels are limited and their use results in global warming due to the emission of greenhouse gases (GHGs). To provide sustainable power production and continuous power resources for future generations, there is a growing demand for energy from renewable sources, such as solar, wind, geothermal, and ocean tidal waves [2]. Renewable energy (RE) sources are the best-proven sources of energy. Solar energy is one of the most abundant resources of RE [3]. Energy from the sun is perceptibly environmentally advantageous in all respects. There are many different ways of generating electricity from the sun's energy. The most popular are photovoltaic (PV) panels, where silicon solar cells convert solar radiation to electricity. The power incident on a PV module depends on the power in the sunlight and the angle between the module and the sun [4]. Keeping the PV-panels perpendicular to the sun's radiation maximizes the output. The systems that are utilized for this movement are called solar trackers [5]. This is because photovoltaic cells mounted at fixed positions do not capture enough sunlight, compared to photovoltaic cells mounted on a solar tracking system. Therefore, researchers have proposed the design of time-based solar trackers. Time-based solar tracking automatically adjusts the solar panel's position to a more optimum position based on time, with the help of a servo motor connected to the solar panel [6]. This tracking movement is achieved by coupling a servo motor to the solar panel, such that the panel maintains its face always perpendicular to the sun, to generate maximum energy [7]. This is achieved by using a microcontroller to send signals to the servo motor which aids in positioning the servo motor carrying the solar panel in a direction perpendicular to the sun.

The solar tracking systems can be passive or active solar tracking systems, these tracking systems can track the sunbeam in one direction (single) axis tracking or two directions (dual) axis tracking. One passive solar tracking system was proposed by [8] who designed and tested a single axis passive solar tracker with shape memory alloy (SMA) actuators. The shape of the actuator was dependent on the temperature of the sun. It was concluded that the efficiency of these actuators was almost 2% and is approximately two orders of magnitude higher than that of bimetallic actuators. Similarly, [9] designed a novel passive tracking system for equatorial regions with an efficiency gain of 23% over traditional fixed PV modules. The design incorporated two bimetallic strips (bulkheads) made of aluminium and steel. Alternatively, [10] designed an active system, which presented a one-axis sun tracking system utilizing three light-dependent resistors (LDRs). The output signals from the three LDRs were fed to an electronic control system which actuated a low-speed 12V DC motor in such a way as to rotate the collector such that it remained pointed toward the sun. Similarly, [11] constructed an electronically one-axis concentrating collector with an electric motor for forced circulation. The collector was hinged at two points for its tilt adjustment with a tightening screw to continuously track the sun from east to west through a range of 180^o. It was concluded that the collector efficiency increases (reaching the maximum value of 62%) as the mass flow rate increases. [12] presented a smart dual-axis solar tracker regarding the dual-axis system. They used Arduino Uno for the development of their proposed model. After the experiment, they observed that maximum voltage was tracked from about 25% to 30% and the generating power increased by 30% compared to the static system. Similarly, [12] investigated dual-axis solar tracking with power energy development compared to a fixed PV panel in Sanliurfa, Turkey. They found that everyday power gain is 29.3% in solar radiation and 34.6% in power generation for a particular day in July. Several regions of the world have recorded varying performance measurements with solar tracker panel and therefore correlates with the varying degree of the sun's intensity across these regions. In Nigeria which falls in the equatorial region of the world with a high degree of the sun's intensity, the implementation of the solar tracker panel is not popular. In addition, the active dual-axis solar tracker can be implemented at a relatively low cost as shown in [13] which was implemented in Morocco. This can boost the popularity of solar tracker panels as an alternative source of electrical energy. Thus, the study aims to build a dual-axis microcontroller-based solar tracking system that compares its performance over the traditional and popular static solar panel as well as investigate the cost of its implementation. Moreover, the authors of [13] explored an add-on for Microsoft Excel, PLX-DAX which allows any microcontroller connected to the serial port of a computer to send data directly into Excel. The features it has range from real-time plots showing time in the format HH:MM:SS recorded at up to 26 columns per frame to read/write privileges on the cells and much more. However, the add-on only works for Microsoft Office/Excel 200 to 2003 and is no longer supported. Alternatively, we used a web app developed in JavaScript to implement the real-time storage of received data over Wi-Fi.

2.0. Materials and Method

The system being proposed involves five components; an ATMEGA328P microcontroller, an internet of things module to display results, the solar panels (static panel and the solar tracker panel), and the light-dependent resistors (LDRs), servo motors and the current sensors. The block diagram of the entire system is given in Figure 1.

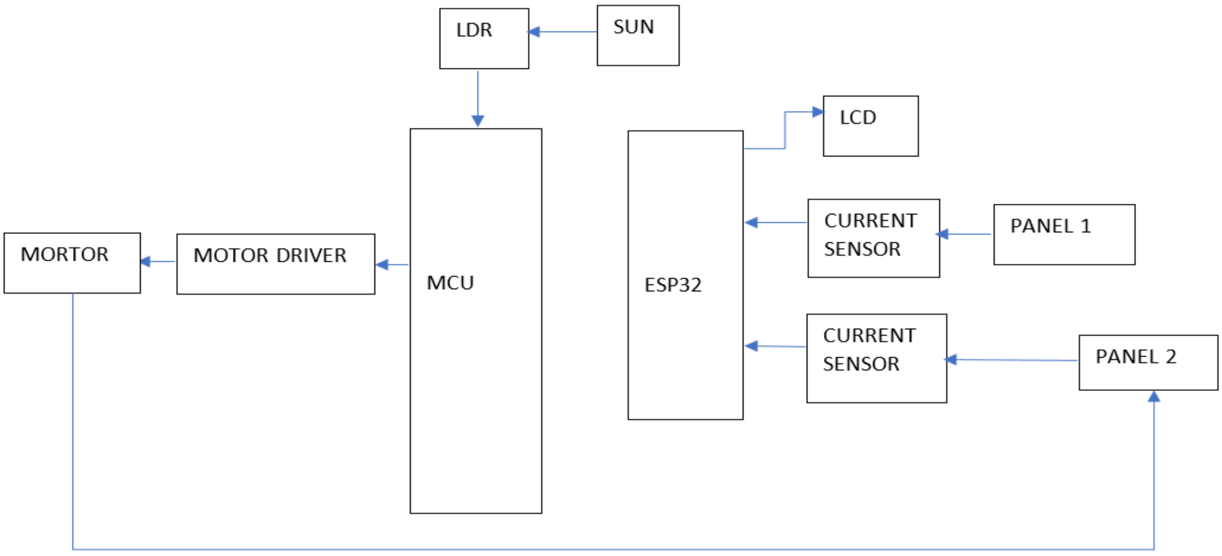

Figure 1. Block diagram of the microcontroller-based solar tracking system

The solar panel is attached to the servo motor which is interfaced with the microcontroller ATMEGA328P. The light-dependent resistor detects the direction with maximum sunlight intensity and sends signals to the microcontroller unit, which will position the motor driver in the direction of maximum light intensity. The current sensor measures the current in both the static solar panel and the solar tracker panel and sends the result to the web application via the internet of things module (ESP Wi-Fi module) to compare the effectiveness of the solar tracker system over the static solar panel system. The overall system has the intended goal of comparing the efficiency of the solar tracker-assisted solar panel and the traditional static solar panel. A web application has been built using JavaScript programming language to receive and store data values current across the day.

2.1. Microcontroller

The microcontroller is a small computer on an integrated circuit that is responsible for the coordination of all operations of the entire system. The microcontroller receives data from the load cells and ultrasonic sensor and process them into readable data and then displays them on the liquid crystal (LCD). Table 1 shows the features of the ATMEGA328P microcontroller that was used and the schematic diagram is shown in Figure 2.

Table 1 Features of the ATMEGA328P microcontroller

Parameter	Values
Overview	High performance, low power AVR 8bit microcontroller
Instructions	131
Architecture	Advanced RISC
Registers	32 8-bit general purpose
Ports	3 I/O ports
Flash memory	32kB
EEPROM	1kB
SRAM	2kB
A/D	10-bit
Instruction speed	10MIPS at 20MHz
Counters/Timers	3
Peripherals	USART, SPI, I2C and ISP
Programmable I/O lines	23
Operating voltage	1.8—5.5

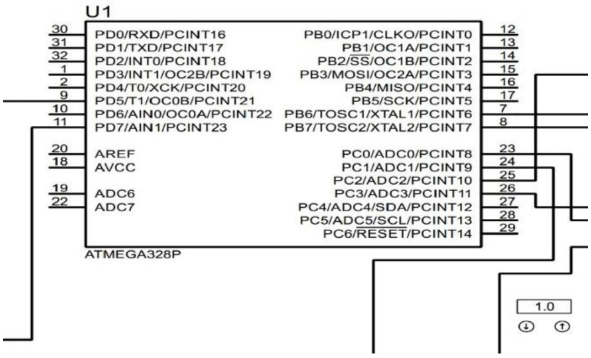

Figure 2. Microcontroller circuit diagram

The safe working operation of the microcontroller is achieved when it is driven by a 16MHz oscillator [14]. Therefore, a 16MHz crystal oscillator was connected to the microcontrollers XTAL 1 and XTAL 2 pins as shown in Figure 3. The microcontroller's instruction execution speed is dependent on the frequency of the crystal oscillator; the higher the crystal oscillator's frequency, the faster the microcontrollers process the command in its memory. The relationship is given by Equation 1.

$$execution\ speed\ = \frac{1}{frequency \times 4\ cycles}\ [15]. \quad (1)$$

At a frequency of 16MHz, the execution speed of the microcontroller can be calculated as $4\ cycles\ \times \frac{1}{16000000}$.

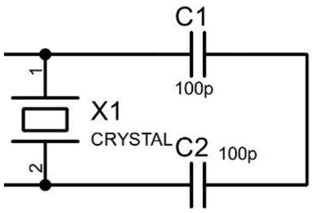

Figure 3. Circuit diagram of the crystal oscillator.

2.2. Buck converter

The buck converter is a DC-DC step-down device used to create a steady DC voltage and current [16]. It is needed to down-convert the 12V supply to the desired rating of voltage required for the microcontroller.

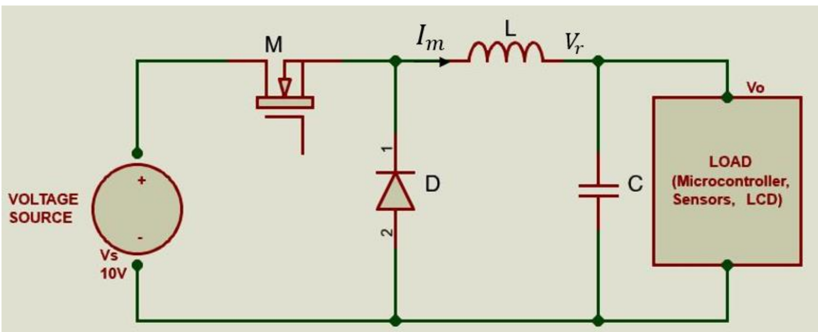

Figure 4. Buck Converter Circuit

At close switch:

Voltage is stepped down while current increases.

I_m = Current across inductor increases.

B_m = Magnetic field across inductor increases.

$$V_r = V_s - V_o. \quad (2)$$

Where V_r = Voltage across the inductor.

V_s = Source voltage and

V_o = output voltage across the load resistor.

$$V_o = V_s(D). \quad (3)$$

D = duty cycle $\left(\frac{time\ when\ the\ switch\ is\ closed}{time\ for\ one\ complete\ cycle}\right)$ which is given as Equation (4)

$$D = \frac{t}{T} \quad (4)$$

Let $t = 1ms,\ T = 2ms,\ V_s = 10V = V_{DC}$. From Equation (4) $D = 0.5$ then from Equation (3) the output voltage is $V_o = V_s \times D$ = 5V.

2.3. Light-dependent resistors (LDRs) and Servo Motor

Light-dependent resistors also known as photoresistors are electronic components used to detect light and change the operation of a circuit depending on the intensity of the light while a servo motor is a rotary actuator that allows for precise control of the angular position. For the automatic solar tracking system, a modular approach was used to control the solar panel at two axes by using four light-dependent resistors (LDRs) as sensors as shown by the circuit representation in Figure 5. The signals from sensors received by the controller are used to determine the direction of movement to align with the rays of the sun. Two servo motors were used to perform this movement based on the signal received from the controller. The panel could rotate at a total degree of 90^o on the vertical level and 180^o on the horizontal level. The schematic diagram of the servo motors is shown in Figure 6.

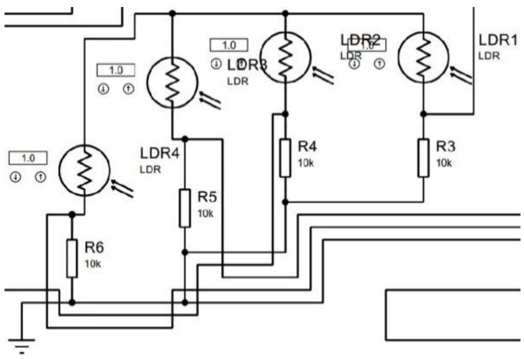

Figure 5 Circuit diagram of the light-dependent resistor.

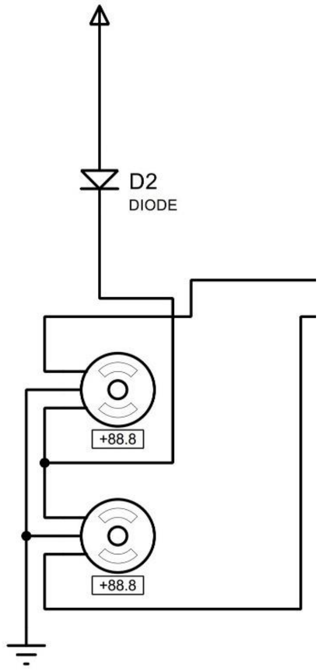

Figure 6 Circuit representation of the servo motor.

During the day, the resistance R_2 of an LDR was assumed to be measured 7at 00Ω, the appropriate variable resistor R_1 suitable for use in the circuit was chosen to be 10000Ω, input voltage V_1 is 5V. Applying the voltage divider rule to the circuit:

Output voltage $V_2 = V_1\ (R_2\ /\ (R_1 + R_2))$ (5)

Hence the divide voltage V_2 = 5 (700 / (10000+700)) = 0.327V.

At night, the variable resistor R_1 decreases to let's say 350ohms and from Equation (5) $V_2 = 5\left(\frac{700}{350+700}\right)$ = 3.33V.

2.4. Fixing the light-dependent resistor (LDR) sensors

The PV panel which was used in the experiment had a rating of 5 Watt and 520mA. To command the PV panel motion, four light intensity sensors were used. The tracking sensor is composed of four similar LDR sensors, which are located at the four corners of the panel to detect the light source intensity in the four orientations. The four sensors are divided into two groups, east/west and north/south. In the east/west group, the east and west LDR sensors compared the intensity of received light in the east and west. If the sensors receive light source intensities differently, the system obtains signals from the sensors' output value in the two orientations. Based on the sensor output value, the system then determines which sensor received more intensive light. The system drives the stepper motor towards the orientation of this sensor. If the output values of the two sensors are equal, the output difference is zero and the motor's drive voltage is zero, which means the system has tracked the current position of the sun. The north/south sensors track the position of the sun similarly.

The LDR helps in actualising the current comparison between the fixed panel and solar panel by the simple Ohms law given in Equation (6).

$$I = \frac{\text{Vs}}{\text{Rd}}. \quad (6)$$

Where V_s is the constant voltage (5V), R_d is the resistance from the LDR that varies with time, and I is the current generated by the solar panel with time.

2.5. Liquid crystal display (LCD)

2.5. The LCD is used for displaying alphanumeric characters and allows for good design. The system that was designed used a 20×4 LCD module connected in the 8-mode as shown in Figure 7.

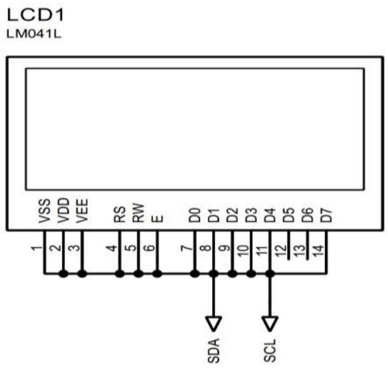

Figure 7 Circuit diagram of the liquid crystal display

2.6. ESP12-F Wi-Fi module

This is a series of low-cost, low-power systems on a chip microcontroller with integrated Wi-Fi and dual-mode Bluetooth. The specifications of the IoT module, ESP-12F are given in Table 2 and the schematic circuit is shown in Figure 8.

Table 2 Specifications of the ESP-12F

Parameter	Value
Protocol	802.11 b/g/n
Serial/UART baud rate	115200 bps
TCP/IP protocol stack	Yes
Operating voltage	3.3V (maximum of 3.6V)

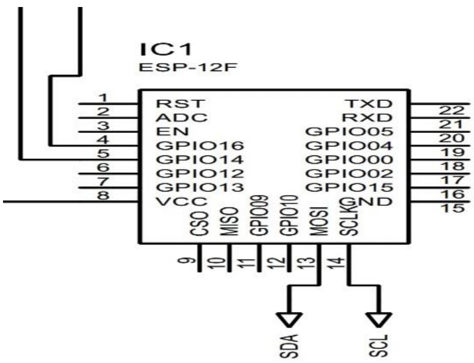

Figure 8 Circuit diagram of ESP32.

The Wi-Fi module is interfaced with the microcontroller to allow data logging. The data gotten from the system is logged into a web server facilitated by a web application that was built using JavaScript. When the variation in current has been evaluated by the microcontroller unit, the equivalent result is sent through the Wi-Fi module to the web server, where it is finally stored.

2.7. Software development

The Arduino Integrated Development Environment (IDE) was used for the development of the firmware for the microcontroller. It is a cross-platform application that is written in C and C++. It is used to write and upload programs to Arduino-compatible boards, but also, with the help of third-party cores, other vendor development boards. The flowchart used for the development of the program is shown in Figure 9.

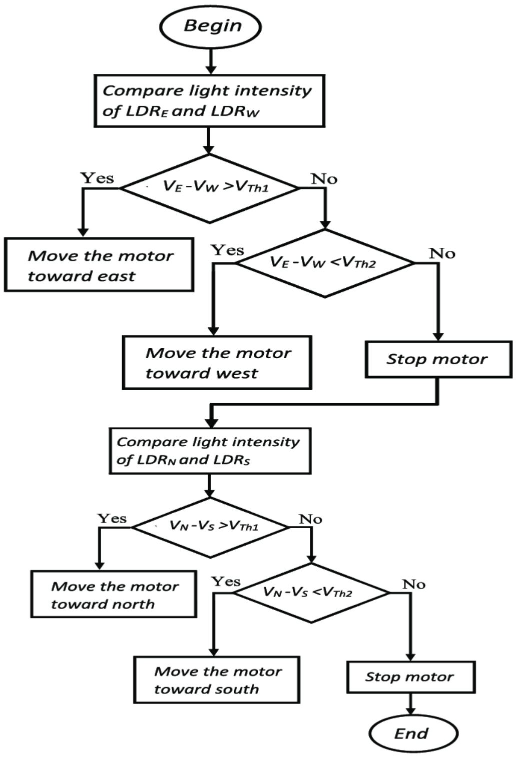

Figure 9 operation of solar tracker [17]

The first step in the program is to initialize all the variables. Next, the program compares the west/east group of LDRs against a pre-defined threshold. If the difference between the voltage across the west/east group of LDRs is greater than the threshold, the west/east group of LDRs are compared with another threshold which determines whether to move the motor westward or stop the motor and in contrast, the motor would move eastward. If the motor stops then, it proceeds to compare the north/south group of LDRs and repeats a similar comparison of the group against predefined threshold values. The complete circuit diagram of the solar tracker is shown in Figure 10.

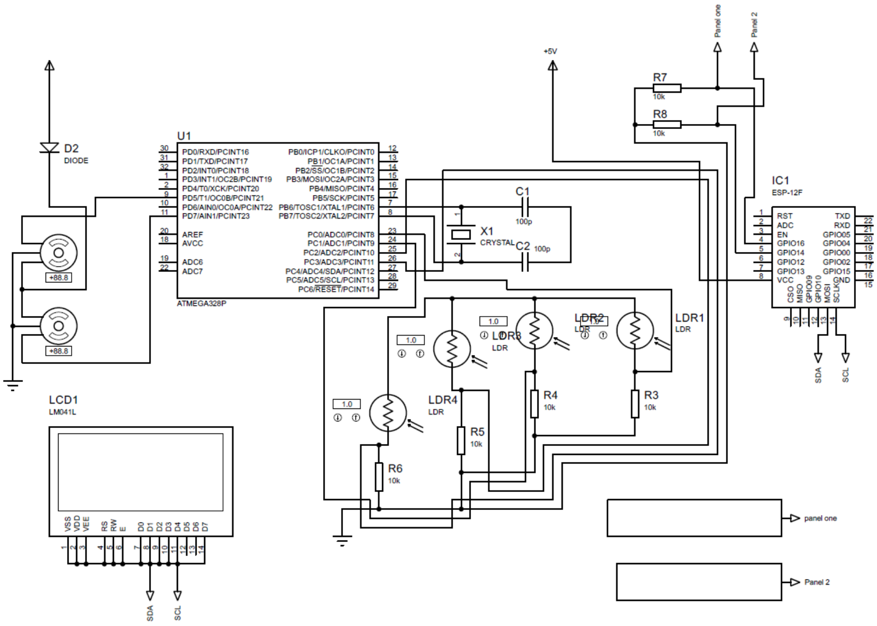

Figure 10 Solar Tracker Circuit Diagram

3. Results and Discussion

The experiment was conducted from 20th May to 9th June 2021 and during that period several weather conditions were experienced. The weather conditions ranged from sunny, to partly cloudy, to very cloudy and raining. The period the experiment was conducted was a season with more rain and cloudy days than sunny days. Thus, the results of the solar tracker were recorded and will be analysed in this section. When the experiment was conducted, the fixed panel and the solar tracker panel were positioned side by side with adequate space between them. The current values of both panels were measured as shown in Table 4.

Table 3 shows the hourly values of current (I) of the tracking and fixed panels, for a period ranging from 8 am to 6 pm from 20th May to 10th June 2021 (20 days intervals).

For every day the experiment was conducted and the current readings of the fixed panel and the solar tracker panel were recorded. The result shown in Table 4 is the entire readings collected from the experiment for 20 days however, it doesn't show the weather on the days the measurements were carried out. There were 3 rainy days, 11 cloudy days and 6 sunny days. Let's observe the hourly plot of the currents of the two panels for the different days; sunny, cloudy and rainy days. Table 6 shows the hourly results of current values for both panels on a sunny day and the results are plotted in Figure 7.

On a sunny day, it was taken in the observation that the solar tracker panel produced a current in the range of 41 to 193 milliampere compared to a lower range by the fixed panel. The high range is a result of the tracker always being positioned in the direction of maximum sun intensity. It was also discovered that the fixed panel had its maximum values from 12 noon to 6 pm.

On a cloudy day, it was observed that the variations in the values of the solar tracker panel and the fixed were dependent on the level of cloudiness. When it was extremely cloudy, the variations become negligible and when it was a little bit cloudy, the variations become a little bit obvious. Table 6 shows the hourly result of current values of both panels on a cloudy day and Figure 12 is the corresponding plot of the results.

DAYS		8 AM	9 AM	10 AM	11 AM	12 PM	1 PM	2 PM	3 PM	4 PM	5 PM	6 PM	Average
20th May	FIXED	3	5	43	55	65	74	72	71	68	70	60	53.27273
	TRACKER	12	51	57	59	67	55	47	45	39	41	32	45.90909
21st May	FIXED	1	53	73	75	80	153	177	176	180	172	166	118.7273
	TRACKER	41	59	81	82	87	132	182	183	193	190	176	127.8182
22nd May	FIXED	0	44	45	47	57	67	187	190	210	208	110	105.9091
	TRACKER	42	46	49	57	68	76	176	187	198	200	168	115.1818
23rd May	FIXED	47	48	55	67	68	68	67	100	103	105	120	77.09091
	TRACKER	0	49	72	76	78	79	77	97	105	109	190	84.72727
24th May	FIXED	2	50	52	54	56	68	68	75	76	72	70	58.45455
	TRACKER	45	60	71	75	76	80	81	86	87	82	83	75.09091
25th May	FIXED	1	16	47	46	48	67	65	67	145	175	85	69.27273
	TRACKER	45	46	55	58	67	83	75	93	160	180	73	85
26th May	FIXED	1	2	6	12	13	5	8	8	14	12	10	8.272727
	TRACKER	3	3	7	14	15	7	10	13	17	14	14	10.63636
27th May	FIXED	2	7	50	90	92	83	140	141	99	76	59	76.27273
	TRACKER	43	56	53	110	140	197	187	167	140	87	61	112.8182
28th May	FIXED	1	3	32	23	13	27	38	98	92	102	90	47.18182
	TRACKER	3	4	36	32	15	28	40	109	110	120	98	54.09091
29th May	FIXED	0	5	15	177	14	23	29	45	67	120	90	53.18182
	TRACKER	4	7	150	170	244	37	32	63	88	150	120	96.81818
30th May	FIXED	0	7	21	65	68	67	89	120	140	220	150	86.09091
	TRACKER	2	9	87	79	89	92	110	150	170	230	167	107.7273
1st June	FIXED	0	8	19	67	67	65	57	30	42	30	23	37.09091
	TRACKER	4	65	78	74	71	69	67	40	45	33	27	52.09091
2nd June	FIXED	0	6	16	55	89	123	140	210	208	210	100	105.1818
	TRACKER	3	7	66	67	101	145	165	237	227	223	109	122.7273
3rd June	FIXED	0	0	4	49	48	45	47	51	120	100	73	48.81818
	TRACKER	2	3	61	69	61	51	64	67	127	108	74	62.45455
4th June	FIXED	1	3	3	54	56	67	183	197	201	130	110	91.36364
	TRACKER	5	5	54	63	64	71	206	207	207	141	121	104

5th June	FIXED	0	8	0	49	57	62	102	111	110	107	89	63.18182
	TRACKER	3	13	62	67	79	82	130	129	120	110	98	81.18182
6th June	FIXED	0	0	0	87	97	87	88	105	107	110	64	67.72727
	TRACKER	3	2	97	112	116	103	114	115	118	118	68	87.81818
7th June	FIXED	1	7	17	78	87	88	86	89	91	97	71	64.72727
	TRACKER	4	12	83	99	109	107	101	103	118	120	78	84.90909
8th June	FIXED	1	6	14	89	99	145	189	189	190	190	170	116.5455
	TRACKER	2	8	98	113	134	166	193	201	203	200	183	136.4545
9th June	FIXED	0	7	13	48	47	43	67	69	73	77	140	53.09091
	TRACKER	3	9	60	61	62	63	92	91	95	99	193	75.27273

Table 4 shows the hourly results of the current values (I_{oc}) of both tracking solar panel and fixed solar panel

21st May	**8 AM**	**9 AM**	**10 AM**	**11 AM**	**12 PM**	**1 PM**	**2 PM**	**3 PM**	**4 PM**	**5 PM**	**6 PM**	**AVERAGE**	**STANDARD DEVIATION**
FIXED	1	53	73	75	80	153	177	176	180	172	166	118.7273	50.11437
TRACKER	41	59	81	82	87	132	182	183	193	190	176	127.8182	51.35611

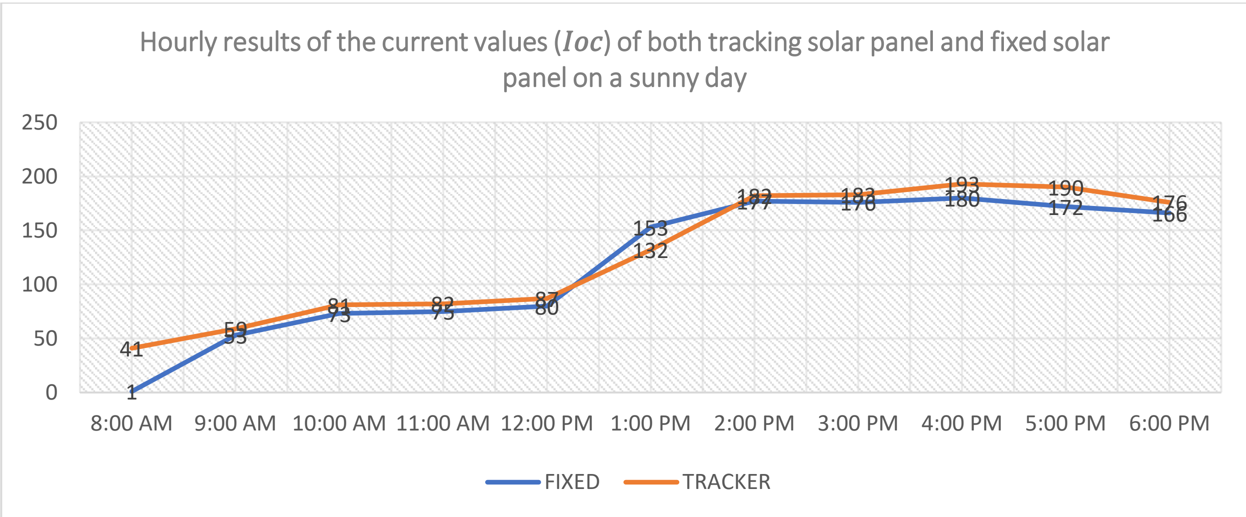

Figure 11 Current comparison between tracking and fixed panels for a sunny day

Table 5 Hourly result of the current values of the fixed and tracker panel on a cloudy day

3rd June	8 AM	9 AM	10 AM	11 AM	12 PM	1 PM	2 PM	3 PM	4 PM	5 PM	6 PM	AVERAGE	STANDARD DEVIATION
FIXED	0	0	4	49	48	45	47	51	120	100	73	48.81818	35.28187
TRACKER	2	3	61	69	61	51	64	67	127	108	74	62.45455	31.21618

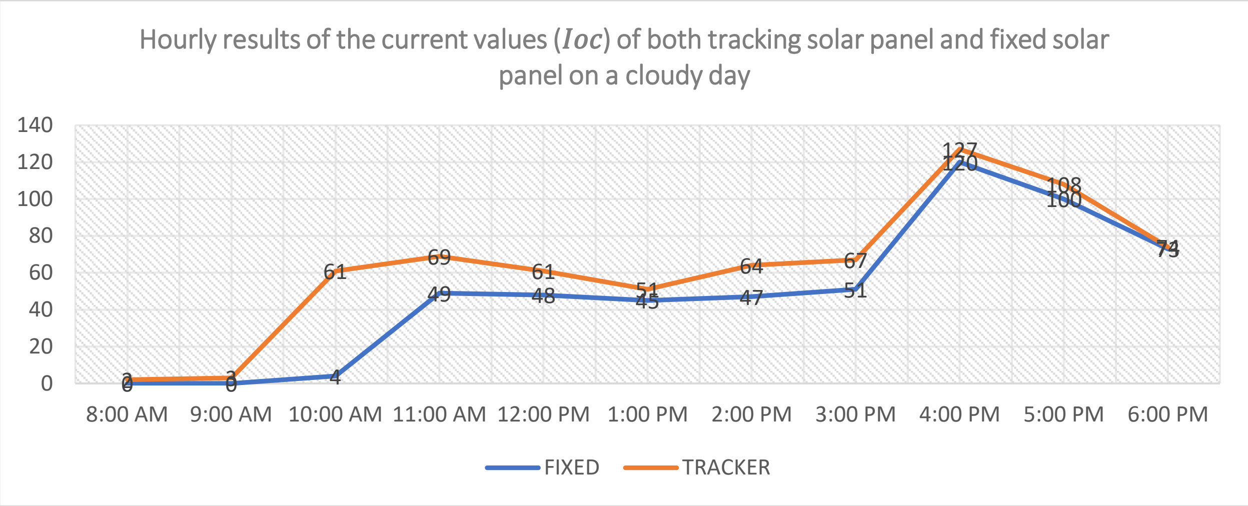

Figure 12 Current comparison between tracking and fixed panels for a cloudy day

On a rainy day, it was observed that the solar tracker and the fixed panel produced almost equal results throughout the day. Table 7 is the hourly results of the current values of the tracker and fixed panel for a rainy day and Figure 13 is the corresponding plot.

Table 6 Current comparison between tracking and fixed panels for a rainy day

26th May	8 AM	9 AM	10 AM	11 AM	12 PM	1 PM	2 PM	3 PM	4 PM	5 PM	6 PM	AVERAGE	STANDARD DEVIATION
FIXED	1	2	6	12	13	5	8	8	14	12	10	8.272727	3.687818
TRACKER	3	3	7	14	15	7	10	13	17	14	14	10.63636	4.223742

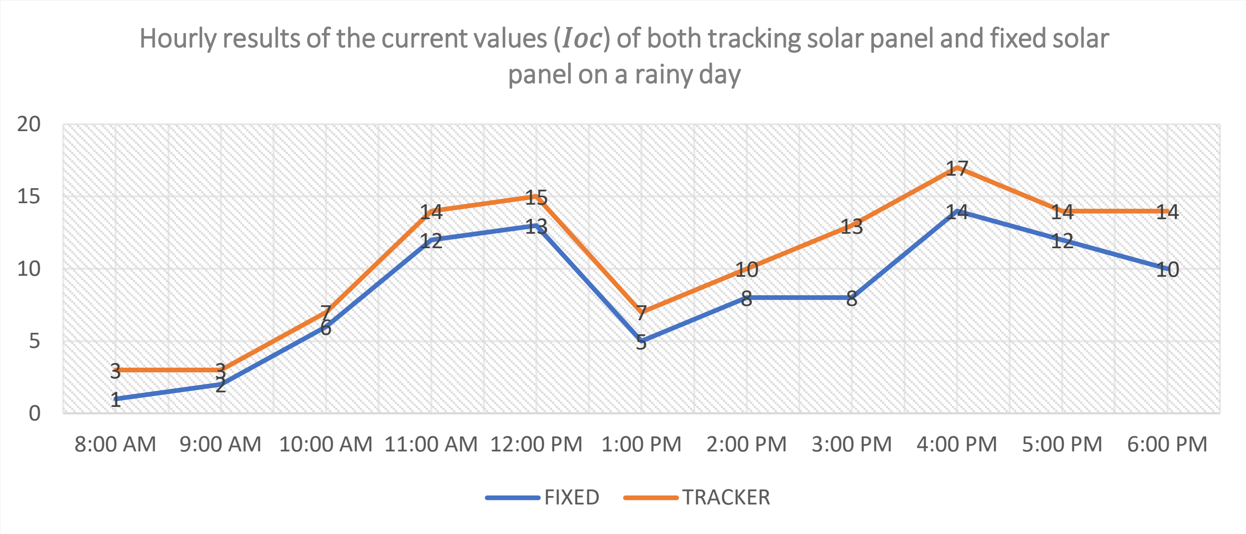

Figure 13 Current comparison between tracking and fixed panels for a cloudy day

3.1. The efficiency of solar panels

The efficiency of each panel was calculated by comparing the current measured from the solar tracker versus that produced by the fixed panel for each day [13]. Table 8 presents a simplified analysis of the data collected for the 20 days showing the average of average and sum of currents for the solar tracker and fixed panel recorded on the sunny, cloudy and rainy days as well as the efficiency performance on those days.

Table 7. Average current and efficiency of PV panels for the selected day.

DAY CONDITION	PANEL	MEASUREMENT OF THE ENTIRE DAY			
		AVERAGE CURRENT OUTPUT (I_{av})	AVERAGE CURRENT (I_{av})	SUM OF OUTPUT	EFFICIENCY (%)
SUNNY	TRACKER	101.4545567	1116		19%
	FIXED	120.45455	1325		
CLOUDY	TRACKER	63.09917455	694.09091		28%
	FIXED	81.03305818	891.36364		
RAINY	TRACKER	32.878789	361.66667		10%
	FIXED	36.21212	398.33333		

It can be observed from the table that when there is a clear sky day the average panel efficiency for the single-axis tracking panel produced an improved efficiency of 19% over the fixed panel. For a cloudy day, the efficiency improved by 28% whereas only a 10% improvement was recorded for cloudy days. Thus, the performance of the solar tracker over the fixed panel for all days was measured at 23%. The results observed by this study correlate with the observations from past researches that show that the single-axis solar tracker can boost the efficiency of a solar system by about 25% to 35% while a dual-axis tracker will boost its efficiency to about 40% to 45%. With a dual-axis solar tracker, the performance is expected to improve beyond that observed in this study. In terms of cost, the table of the bill of material in the Appendix shows a relatively low-cost implementation as it cost below 240 USD (100000 NGN). This should constitute a low-cost implementation if unnecessary components are excluded from the cost.

4. Conclusion

The study successfully designed and compared the efficiencies of the fixed and solar tracker panels. To achieve this, a single-axis microcontroller-based solar tracker was designed and constructed to control the solar panel to the angle where the maximum radiation from the sun. In comparison to the popular traditional solar panels. It was observed that the use of the single-axis solar tracker improves the overall efficiency of the PV cells by about 23%.

Acknowledgment

The authors wish to acknowledge the assistance and contributions of the project student of the Department of Electrical/Electronic Engineering, Faculty of Engineering, University of Benin, Benin City toward the success of this work.

Conflict of Interest

There is no conflict of interest associated with this work.

References

[1] S. P. Kuchekar, "Solar Tracking System For An Automated Water Pump.". Jounal of Ambient Energy Vol. 34p3-9 2018

[2] S. K. Jain, R. Misra, A. Kumar and G. D. Agrawal, "Thermal performance investigation of a solar air heater having discrete V-shaped perforated baffles," *International Journal of Ambient Energy,* vol. 43, p. 243–251, July 2019.

[3] A. Ponniran, A. Hashim and H. A. Munir, "A design of single axis sun tracking system," pp. 107-110, June 2011.

[4] V. Lindberg and J.-P. Mäki, "SKF dual axis solar tracker-From concept to product," 2010.

[5] K. Vyas and S. Jain, "Development of Automatic PV Power Pack Servo Based Single Axis Solar Tracking System," *IOSR Journal of Electrical and Electronics Engineering (IOSR-JEEE),* vol. 10, p. 7–10, 2015.

[6] M. Lab, "Time based solar tracking system using microcontroller.," 2017. [Online]. Available: https://microcontrollerslab.com/time-based-solar-tracking-system-using-microcontroller/. [Accessed 19 03 2022].

[7] M. J. Rivero, E. Bringas, A. Dominguez and I. Ortiz, "Chemical Engineering European Project Semester: an international proposal for teaching Chemical Engineering," *@tic. revista d\textquotesingleinnovació educativa,* vol. 0, December 2014.

[8] V. Poulek, "Testing the new solar tracker with shape memory alloy actors," in *Proceedings of 1994 IEEE 1st World Conference on Photovoltaic Energy Conversion-WCPEC (A Joint Conference of PVSC, PVSEC and PSEC),* 1994.

[9] M. J. Clifford and D. Eastwood, "Design of a novel passive solar tracker," *Solar Energy,* vol. 77, p. 269–280, 2004.

[10] S. A. Kalogirou, "Design and construction of a one-axis sun-tracking system," *Solar energy,* vol. 57, p. 465–469, 1996.

[11] S. M. A. Ibrahim, "The forced circulation performance of a sun tracking parabolic concentrator collector," *Renewable energy,* vol. 9, p. 568–571, 1996.

[12] M. Kacira, M. Simsek, Y. Babur and S. Demirkol, "Determining optimum tilt angles and orientations of photovoltaic panels in Sanliurfa, Turkey," *Renewable energy,* vol. 29, p. 1265–1275, 2004.

[13] A. E. Hammoumi, S. M. Abdelaziz, E. Ghzizal, A. Chalh and A. Derouich, "A simple and low-cost dual-axis solar tracker," *Energy Science and Engineering,* vol. 6, no. 5, pp. 607-620, 2018.

[14] D. ATMEGA328P, "Atmel Corporation," *San Jose, CA,* 2008.

[15] S. Borah, R. Kumar and S. Mukherjee, "Low-cost IoT framework for irrigation monitoring and control," *International Journal of Intelligent Unmanned Systems,* 2020.

[16] J. Ejury, "Buck converter design," *Infineon Technologies North America (TFNA) Corn Desion Note,* vol. 1, 2013.

[17] S. Karthik, P. V. Karthick, R. R. Thirrunavukkarasu, S. S. Kumar and D. Selvakumar, "Smart Solar Panel using Light Dependent Resistors," in *IOP Conference Series: Materials Science and Engineering*, 2020.

[18] L. P. P. R. K. Dhanalakshmi.V, "Dual Axis Solar Tracker Using Arduino Uno," *International Journal on Recent and Innovation Trends in Computing and Communication,* vol. 4, no. 6, pp. 386-388, 2016.

Appendix

Table A1: BEME of the materials and equipment used

S/N	DESCRIPTION OF ITEM	QUANTITY	UNIT	RATE(Naira)	AMOUNT
1	Solar Panels	2	Nos	6000	12000
2	capacitors	1	Nos	50	50
3	Microtron controller (ATME328)	1	No	5000	5000
4	Motor driver circuit	1	No	1500	1500
5	Servo Motor	2	No	5000	10000
6	Resistors	5	No	50	250
7	Jumper wires	1	rows	1000	1000
8	Breadboards	1	No	500	500
9	Solar wires	3	yard	650	1900
10	Photoresistors	4	Nos	250	1000
11	Veroboard	1	No	200	200
12	Casing	1	no	400	400
13	3D printing	-	-	-	5000
14	ESP32 Wi-Fi module	1	no	5300	5300
15	Service Charges		-	-	40000
16	Screws	4	no	10	40
16	Total	-	-	-	73340